Plasma Research Express

PAPER

Melting transition of two-dimensional complex plasma crystal in the DC glow discharge

Plasma Research Express

PAPER

Melting transition of two-dimensional complex plasma crystal in the DC glow discharge

RECEIVED
21 March 2019

REVISED
29 April 2019

ACCEPTED FOR PUBLICATION
3 May 2019

PUBLISHED
26 June 2019

S Jaiswal and E Thomas Jr

Physics Department, Auburn University, Auburn, Alabama 36849, United States of America

E-mail: surabhijaiswal73@gmail.com

Keywords: DC glow discharge, dusty plasma, coulomb crystal

Abstract

The formation of self-consistent dust crystal and its melting is a well- known phenomenon in rf generated plasmas but remains challenging in DC glow discharge plasmas. Here, we report the melting of a two- dimensional dusty plasma crystal, suspended in the cathode sheath of a DC glow discharge plasma. The experiments are carried out in a Dusty Plasma Experimental (DPEx) device which consists of a circular powered electrode and an extended grounded cathode tray. A stationary crystal of melamine formaldehyde particles is formed in a background of Argon plasma between a pair of confining strips that are placed on the cathode. The stable structure breaks and transition to a fluid state when the neutral pressure is reduced. The neutral pressure range where this melting transition is observed is an order of magnitude less than what is typically reported in rf discharge plasma. The transition is confirmed by evaluating the variation in different characteristic parameters such as the pair correlation function, Voronoi diagram, local bond order parameter, defect fraction and dust kinetic temperature as a function of background neutral pressure. For instance, the average bond order parameter (Ψ_6) reduces from 0.87 to 0.4 when the neutral pressure is reduced from 15 to 11 Pa. The asymmetry of the electrode is a special feature that is believed to enable the formation of the plasma crystal.

1. Introduction

'Dusty' or 'complex' plasmas are composed of the usual combination of electrons, ions, neutral atoms and the charged, dust particulates of micron or submicron size. These particles are either added to the plasma or grown in the plasma by sputtering or by polymerization and agglomeration of reactive gases. Under typical low temperature laboratory conditions with electron temperature $T_e < 5$ eV and room temperature ions, the particles become negatively charged by collecting more electrons than ions and then act as a third charged component in the plasma- adding more richness to the collective dynamics of the system. Their existence in astrophysical situations such as planetary rings, comet tails, interplanetary media, and interstellar clouds [1, 2] as well as various industrial application [3] has made the study of dusty/complex plasmas an active area of research for the last few decades [4, 5]. The highly charged dust cloud in the laboratory plasma levitates near the sheath boundary by balancing the gravitational force on the dust grains against the electrostatic force arising from the sheath electric field. The dust particles also interact among themselves through their mutual Coulomb repulsion and, under the appropriate conditions, can form a self-organized, strongly coupled system. The strength of coupling can be characterized by a coupling parameter Γ, which is the ratio of the interparticle coulomb potential energy to the dust thermal energy. When Γ exceeds a critical value, the system forms a regular lattice structure so-called Coulomb crystal. The necessary plasma condition for the dust crystal formation was first derived by Ikezi *et al* [6] and the experimental observation was first reported in 1994 by Chu *et al* [7] and Thomas *et al* [8]. Control over the coupling strength has made dusty plasmas an excellent platform for studying the phenomenon of phase transition, transport properties of the strongly coupled system and other related topics that have great applicability in a variety of areas such as statistical mechanics, soft condensed matter and colloidal

suspensions. The spatial and time scales of the particle motion allow the dust grains to be directly visualized using laser illumination and high-speed cameras. Further, the weak frictional damping enables the measurement of the dynamics and kinetics of individual particles. This opportunity to have such a detailed diagnosis of a dusty plasma has motivated a great deal of research related to crystal formation, phase transitions of two and three dimensional crystals [9–12], re-crystallization [13], instabilities [14, 15], magnetic field effect on the phase transition[16], heat transport [17, 18] and an extensive list of additional topics.

The majority of experimental studies that have been devoted to the formation of the dust crystal and its melting dynamics has been done using rf discharge plasma. The studies of dust crystal in DC glow discharge plasma are very limited. Among such few works are those of Fortov *et al* [19] and Maiorov *et al* [20]. In both the experiments, a crystalline structure with multiple layers were formed by the trapping of dust particles in the standing strata of a dc glow discharge that appear under weakly ionized conditions in the positive column of a DC glow discharge. However, this method has the limitations that the crystal structure can be formed and sustained over a narrow range of discharge parameter and the strong variation in the electric field leading to small scale inhomogeneities in the particle cloud. Mitic *et al* [21] also studied the formation of a three-dimensional ordered structure in a low frequency quasi DC plasma at discharge conditions where no striations were present. Particle cloud in their experiment were trapped by mitigating the effect of the longitudinal electric field by using an alternating DC current of a frequency of 1kHz. Although these experiments enabled ordered structures to be formed in dc discharges, these experimental arrangements were still found to be insufficient for the observation of a perfect crystal structure. There are two main factors that may be responsible for the difficulty of achieving Coulomb crystallization in dc discharges: (1) reduced charging of the dust particles and (2) excess heating of the dust by ion bombardment. Due to a lower electron density in the sheath of the DC plasma, a particle which immersed deep inside the sheath may not be able to collect as many electrons [4]. As a result, the coupling parameter for the same dust kinetic temperature tends to be relatively lower in the case of DC plasma. Furthermore, the heating of the dust due to the impact of ion streaming may be more effective in the case of parallel electrode arrangement because the ions accelerated by the DC voltage directly impinge on the levitated dust cloud that is formed between the electrodes and could cause its temperature to rise. The limitations on the performance of dc glow discharge plasma may be overcome through an improvement in the geometry of the electrodes so that the direct bombardment of ions on the dust cloud can be restricted. This could overcome the difficulty of the formation of dust crystals in such devices. Recently, the formation of a stable plasma crystal in the DC glow discharge has been observed [22, 23] in the dusty plasma experimental (DPEx) device where an asymmetric electrode arrangement with extra confinement strip/ring is used for particle confinement [24]. However, the phenomenon of the melting transition of dust crystal in DC glow discharge is still unexplored. The detailed investigation of crystalline behaviour and phase transition of dusty plasma in the DC discharge is important for understanding the fundamental physics as well as for production and control of the properties of the dust crystal in different plasma sources.

In this paper, we report on the novel experimental observation of melting transition of two- dimensional dusty plasma Coulomb crystal levitating in the cathode sheath of the DC glow discharge plasma. The experiments have been carried out in the dusty plasma experimental (DPEx) device [24] with a unique electrode configuration that permits investigation of dust Coulomb crystals over a wide range of discharge parameters with excellent particle confinement. The melting is induced by changing the discharge parameter. The phase transition is confirmed by investigating the global and local variation in the structural dynamics of the crystalline structure by calculating the pair correlation function, local bond order parameter and defect fraction. The cause of melting is qualitatively explained by an increasing dust kinetic temperature as a result of the combined effect of ion streaming and charge fluctuation.

The paper is organised as follows: in the following section, in section 2, we describe the experimental arrangement in detail. In section 3, we discuss the experimental results on the formation of the dust crystal and its melting dynamics. A brief concluding remark is made in section 4.

2. Experimental arrangement

The experiments are performed in Dusty Plasma Experimental (DPEx) device which consists of a $\Pi-$shaped pyrex glass tube with a horizontal section of 8 cm inner diameter and 65 cm length. This section is used for all the dusty plasma experiments. The two vertical sections of the same diameter and 30 cm length is used for other functional access such as gas inlet, pumping connection etc. An asymmetric electrode arrangement, consist of a 3 cm stainless steel disc anode and 40 cm $\times$ 6.1 cm $\times$ 0.2 cm cathode tray is used to strike argon plasma. Figure 1 shows the schematic diagram of the experimental arrangement used for the current experiment. A detailed description of the experimental setup and its operational characteristic is reported elsewhere (see [24]).

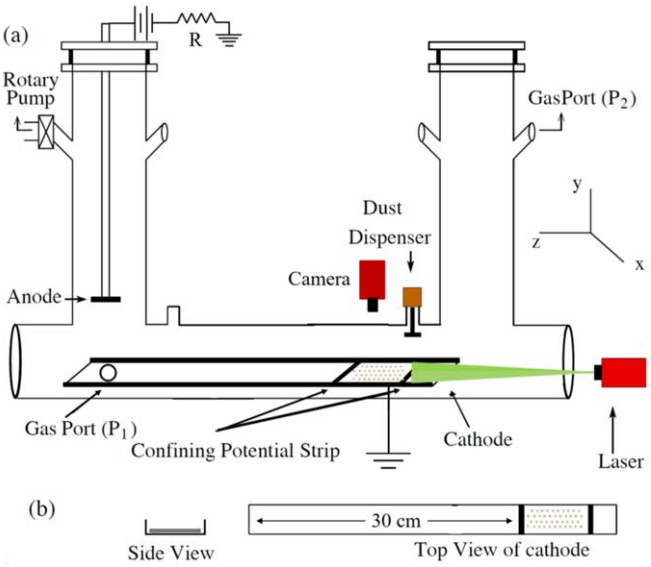

Figure 1. (a) Schematic diagram of Dusty Plasma Experimental (DPEx) setup., R: current limiting resistance. (b) Side and top view of the cathode tray.

The experimental setup is evacuated to a base pressure of 0.1 Pa by a rotary pump. To remove any kind of impurities, Argon gas is then flushed several times and then pumped down to its base pressure. Finally, the working pressure is set in the range of 10–20 Pa by maintaining the pumping speed and the gas flow rate. A DC glow discharge plasma is formed in between the anode and cathode by applying a discharge voltage in the range 310–320 Volts. The corresponding discharge current is in the range of 2–5 mA. Mono-disperse melamine-formaldehyde spheres of diameter 4.38 $\pm$ 0.06 μm are introduced into the plasma by shaking a dust dispenser which is located inside the vacuum vessel. Once introduced into the plasma, these particles become negatively charged by collecting more electrons than ions and trapped in the plasma sheath boundary above the grounded cathode. In this levitating condition, the vertical component of the sheath electric field provides the necessary electrostatic force to the particles to balance the gravitational force. The radial sheath electric fields due to the bending edges of the cathode tray are responsible for the radial confinement of the dust particles against their mutual Coulomb repulsive forces. An important variation in this experimental setup is the addition of two stainless steel strips of 1 cm $\times$ 6 cm, placed at 6 cm apart on the cathode and approximately 30 cm from the anode. The presence of the strips is believed to be a critical feature to provide the confinement of the dust particles in the axial sheath electric field. In this way, a steady-state equilibrium dust cloud is levitated over the cathode in between the two stainless steel strips at a height of $\approx$2 cm. The levitation height and cloud size can be modified by varying the discharge parameters and hence manipulating the sheath around the rectangular region. The axial confinement also influences the dynamics of the streaming ions in a significant manner. A detailed description of such behaviour in DPEx is provided in the study by Hari *et al* [23]. The particle-cloud is illuminated by a horizontally expanded thin sheet of green laser light (532nm, 100 mW) which is sufficiently constricted vertically to study an individual layer of the dust cloud. The Mie-scattered light from the dust particles is captured by a CCD camera (shown in figure 1) at 25 fps with a resolution of 9 μm/pixel and the images are stored into a high—speed computer.

3. Experimental results and discussion

3.1. Crystalline structure formation

We begin the discussion of the experimental results by describing the experimental parameters needed to form the plasma crystal and the initial characterization of the crystal structure. It is found that the formation of the crystal occurred in a very narrow range of experimental parameters of discharge voltage/current and pressure. Small variations led to the disruption of the structure. Therefore, the experiments that are described here will have a fixed voltage of 310 Volts and we will manipulate the experimental conditions by varying the argon neutral pressure. By careful variation in pressure while keeping the voltage fixed we found that the dust cloud settled into a crystalline structure at a pressure of 14 Pascal. A snapshot of Coulomb crystal is shown in figure 2. It is clearly visible that dust particles are arranged into a regular hexagonal lattice with nearly uniform particle spacing and good translational periodicity which illustrates that the system appears to maintain long—range

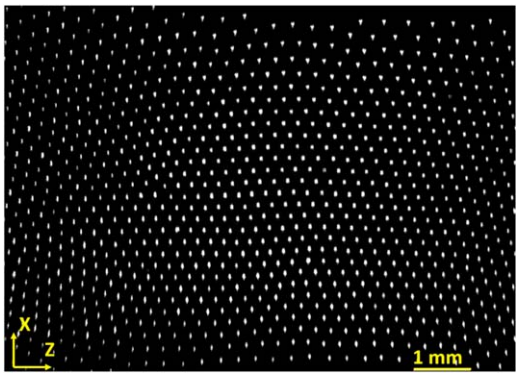

Figure 2. A snapshot of the Coulomb crystal formed at pressure 14 pascal, and discharge voltage of 310 Volt.

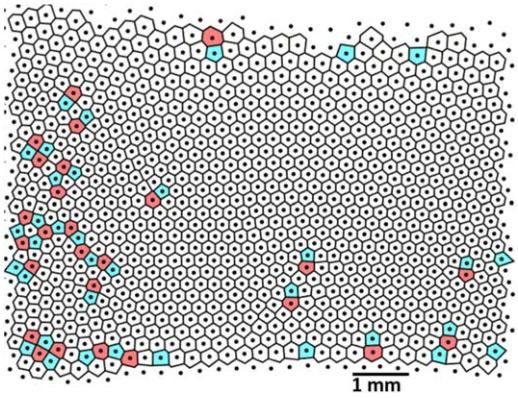

Figure 3. Voronoi diagram of the particle location at P = 14 Pa which is shown in figure 2.

ordering. It is worth mentioning that we have also seen two layers in the dc glow discharge plasma as similar to crystalline structure reported in rf plasma [9]; however, most of the crystal points do not show any deviation. This indicates that particles are almost perfectly aligned in the vertical direction and the lower layer does not appear to have any significant effect on the upper layer. The structure is almost stationary with a small thermal fluctuation around the equilibrium position that we have checked from the overlap of 100 video consecutive frames. In the subsequent experimental analysis, we mainly focus on the topmost layer.

The Voronoi diagram (Wigner-Seitz cell) of figure 2 is shown in figure 3. From this analysis, we can quantify the hexagonal structure and can obtain a rough estimate of the ordering of the crystalline structure. It is seen that most of the cells are six—sided with almost all having the same size. Some of the polygons in the structure have five and seven sides as shown by cyan and red colour in figure 3 which represents a disclination in the crystal. An array of disclinations are visible mostly in the left region of the structure which can lead to defects in the crystal structure. From the Voronoi diagram, it is calculated that 93.2% of the Wigner-Seitz cells are hexagon whereas 3.9% and 2.9% polygon have 5 sides and seven sides respectively. This indicates that the observed structure is a highly ordered crystal with very few defects. Furthermore, the percentage of ordering can be calculated by dividing the number of hexagon to the total number of polygons in the Voronoi diagram. The structural order parameter is estimated as 93%.

We can further estimate the range of positional ordering of the crystalline structure by calculating the radial pair correlation function, g(r). The radial pair correlation function is a measure of the probability of finding the particles at a distance r from the reference particle and can be calculated by directly measuring the average distance between particles. Figure 4 depicts the g(r) vs r of the structure shown in figure 2 where 50 frames have been used for averaging. It can be seen from the figure that the positional order of the structure is preserved upto the sixth nearest neighbour, revealing the presence of a long range ordering and a nearly perfect crystal formation at a pressure of P = 14 Pa. The black vertical lines in the bottom showing the positions of an ideal hexagonal lattice that is in line with corresponding g(r) of the observed crystal. The observed structure is a hexagonal structure also resembles to those reported in an rf plasma by Melzer *et al* [9]. The pair correlation

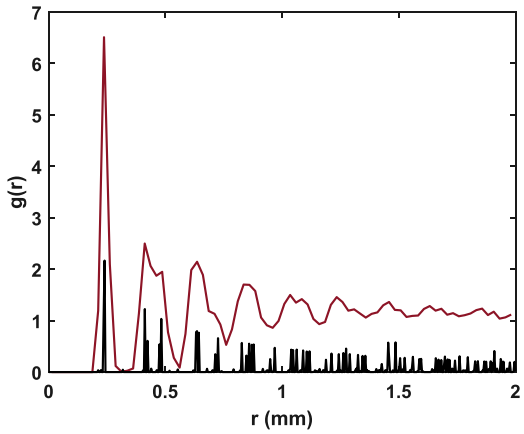

Figure 4. Pair correlation function g(r) of the particle cloud at 14 Pa. The discharge voltage is 310 Volt. The black vertical lines showing the positions for an ideal Hexagonal lattice.

function also provides a good estimate for the mean inter-particle spacing from the position of the first peak. The mean inter-particle distance for the structure in its crystalline states is $\Delta r \sim 250$ micron.

3.2. Structural change of the cloud with changing pressure

In our experiment it has been found that the transition depends on discharge voltage and background pressure. It is noted that small variations in discharge voltage changes the plasma abruptly making it difficult to identify a clear transition from solid to liquid in sequential order. Therefore, as discussed above, the studies described below will focus on using variations of the neutral pressure to control the structural ordering of the particles.

The change in the structure of the particle ordering is investigated as a function of decreasing neutral pressure. In order to understand the melting transition of the dust crystal in DC plasma, we have performed a variety of diagnostic tests on the experimental data in the form of calculating the pair correlation function, defect measurement, calculation of local bond order (Ψ_6) and estimating the dust kinetic temperature. These parameters give information on the global and structural properties of the dust particles.

Keeping the discharge voltage constant at 310 Volts while reducing the background neutral pressure from 15 to 11 Pa in steps of $\Delta P = 1$ Pa, the melting of the particles is characterized. The pair correlation function which, delineate the global system properties in terms of degree of long range order of the distribution of particles, is plotted in figure 5. Figure 5(a) presents the g(r) vs interparticle distance (r) at a pressure of 14 Pa. The nature of the correlation function shows the existence of long range ordering over a distance upto 2 mm with a very pronounced peak which is indicative of the system being in the crystalline state. This can also be confirmed from the splitting of the second peak. With the decrease in pressure, the peaks become shorter and flattered, showing the increasing disorderness of the cloud. Additionally, the number of peaks and the length to which ordering is observable becomes decreased. Figure 5(c) shows the pair correlation function at $P = 12$ Pa and illustrates that the phase state of the particle changes significantly and it tends towards the liquid state with the primary peak followed by a fast descending second or third peak. At a pressure of 11 Pascal, the system becomes almost liquid like as shown in figure 5(d), where only a small hump appears after a primary peak in the correlation function. These pair correlation function measurements indicate a transition from an ordered solid structure to the fluid at lowering pressure. It is quite interesting to note that the stability of the crystalline structure in DC plasma maintained only for a narrow range of background neutral pressure and a transition to disordered state occurs at small variation of discharge parameters; this is unlike the rf plasma where a stable crystal can be maintained over an extended range of pressure variation.

In order to get a deeper insight on melting dynamics of the structure, it is important to understand the local variation in structural dynamics of the particle cloud. This is done by calculating the local bond order parameter and the average defect fraction. These quantities are defined locally and measure the structural properties of the lattice directly at the respective particle positions [25, 26]. A bond order parameter, Ψ_6 examine the lattice in terms of the local orientational order of the particles [26, 27]. For a given particle k, Ψ_6 is defined as

$$\Psi_6(k) = \frac{1}{N}\left|\sum_{n=1}^{N} e^{6i\theta_{kn}}\right|, \tag{1}$$

Here, N is the number of nearest neighbours and θ_{kn} is the angle of the bond between the kth and nth particles with respect to the x-axis. For an ideal hexagonal structure, the bond order parameter is maximum ($\Psi_6 = 1$)

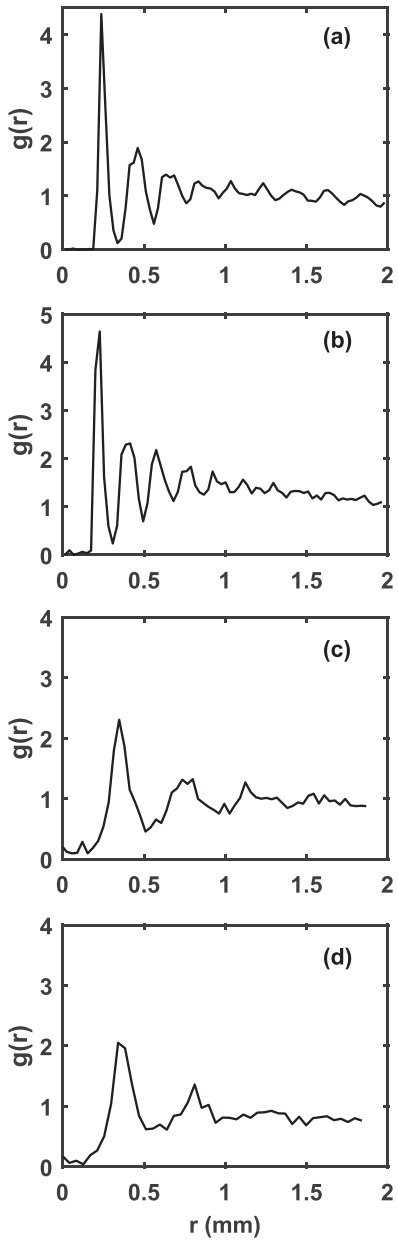

Figure 5. The pair correlation function g(r) of the particle clouds with the changing pressure (a) 14 Pa, (b) 13 Pa, (c) 12 Pa, and (d) 11 Pa.

hence it is a good measure of the deformation of a cell from the perfect hexagon. Lattice sites with nearest neighbour bond angles deviating from 60° will decrease Ψ_6. The same accounts for lattice sites with a number of nearest neighbours other than six. For calculating the bond order parameter, we first identify the particle locations and find out the nearest neighbours of all the particles using Delaunay triangulation. After that, for every particle k, we calculate a vector going to its nearest neighbours n and then calculate the angle of the vector kn with respect to the *x*-axis. A Voronoi map of the particle cloud which is color coded according to Ψ_6 is shown in figure 6. Figure 6(a) presents the Voronoi map corresponding to the pressure of 15 pascal. We can see from the figure that the structure shows a high orientation ordering as most of the Voronoi cell around the particles exhibit perfect hexagonal structure (coloured by blue). Those Voronoi cells which exhibit very low ordering, as visible in the right side of the cloud, cause defects. The number of ~~the~~ cell having lower bond order is seen to be increased as we decrease the pressure to 13 pascal (figure 6(b)) however, the change is not very significant. At a pressure of 11 pascal the cloud loses its orientational ordering completely and almost all the cells manifest a lower bond order as can be seen in figure 6(c). The variation in average bond order parameter, Ψ_6 with pressure is plotted in figure 7. The mean Ψ_6, which is obtained by calculating the $\Psi_6(k)$ for each unit cell and then taking the average over all the cell, gives the information of overall orientational ordering of the system. The local order of the particle cloud is ~0.87 at P = 15 Pa and remains constant down to a pressure of P = 13 Pa. It decreases to

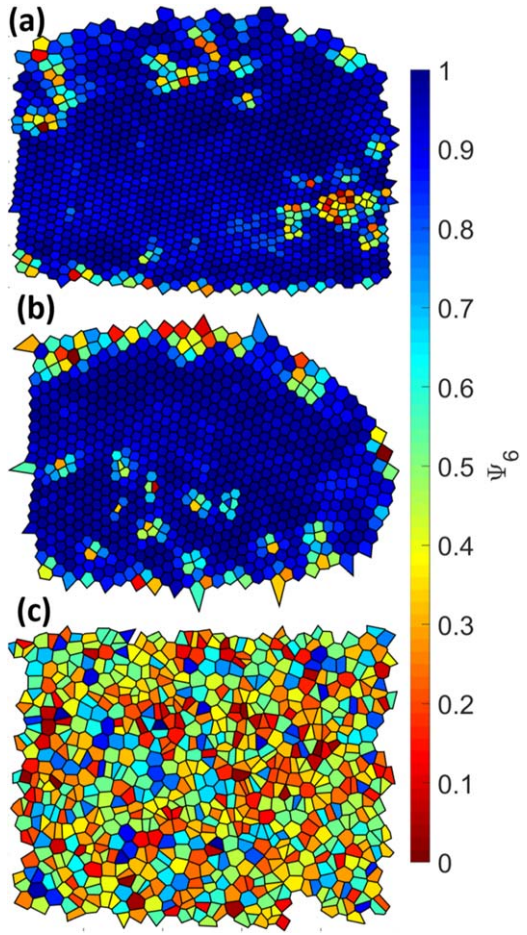

Figure 6. Development of the local order parameter Ψ_6 during the melting transition. (a) corresponds to 15 Pa. (b) 13 Pa and (c) 11 Pa. Unit cells of particles are coloured according to their bond-order parameter.

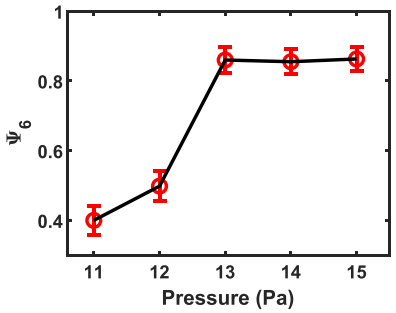

Figure 7. Variation of the average bond order parameter Ψ_6 with pressure.

0.48 when the pressure is reduced to P = 12 Pa and further reduces to 0.4 at P = 11 Pa. This is generally consistent with values reported for the melting dynamics in rf plasmas [26].

We further parameterize the structure by calculating the presence of defects with decreasing pressure. Generally, a defect causes the disorganization of particles in a crystal lattice. Most common defects in the two—dimensional system are point defects or disclinations which arises due to vacancy or an interstitial. A hexagonal lattice with typically six nearest neighbours to each lattice site predominantly encounters two types of point defects namely 'five-folded' or 'seven folded' lattice sites. The other kind of defects that exists in a system are 'free dislocation', which is an additional row of dust particles in an ideal lattice that can be viewed as a pair of a 5-fold and 7-fold disclinations, and dislocation pairs (the quarter of 5-fold and 7-fold disclination). A variety of theories have been reported for rf plasmas that describe the melting transition of dust crystal based on the formation of these defects [9, 10, 26]. The KTHNY theory [9, 26] describes the melting of the crystal lattice by

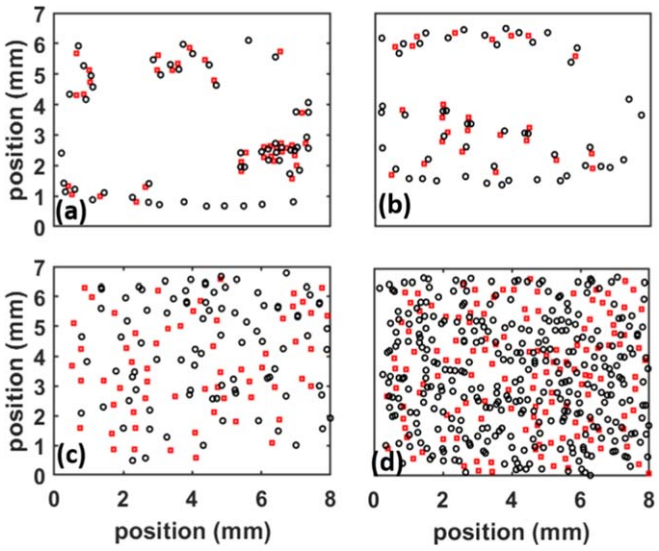

Figure 8. Defect plots for the particle cloud at (a) 15 Pa, (b) 13 Pa (c) 12 Pa and (d) 11 Pa. The discharge voltage is 310 Volt. Square and circle denote the seven—sided polygon and pentagon respectively.

two continuous phase transition in which firstly the dislocation pairs unbind into free dislocations followed by the stage where dislocations (pairs of a 5-fold and 7-fold disclination) breaks into free disclinations. The first stage is called as hexatic phase where positional order is destroyed but orientation order still can be found in the system. In the second stage, the orientation order also disturbed and the liquid state is reached. In our case, we have performed Delaunay triangulation to find out the positions of each particle and locate the nearest neighbour of corresponding particles. We then identify and count the particle having five and seven nearest neighbours respectively. The defect fraction can be calculated by taking the ratio of the number of disclinations (5 or 7 folds) to the total number of particles in a frame.

Figure 8 shows the defect plots at various pressures. The red circles and black squares in the figures mark the locations of 5 and 7-fold defects. At a pressure of 15 pascal (see figure 8(a)) we can see the dislocation pairs but mostly free dislocations can be seen. Some chainlike arrangements of the defects also appear. The defect fraction corresponding to five and seven nearest neighbours are calculated as 4.2% and 2.9% respectively. There is no significant variation found upto 13 pascal with the defect fractions of 6.3% (five nearest neigbours) and 3.2% (seven nearest neigbours). A notable change in the defect fraction is observed as the pressure is further reduced to 12 Pascal and the defect arrange more and more in chains as visible from figure 8(c). The defect fractions in the case are calculated as 30.6% and 20.6% respectively. At 11 Pascal almost all the defect sites correspond to free disclination (figure 8(d)) and defect fraction for 5 fold is calculated as 38% whereas 29% for 7- fold. The observed melting transition does not exactly follow the KTHNY theory of melting. It has been suggested that the type of the melting transition is also sensitive to the number of dust grains in the structure. Therefore, a detailed study of the effect of particle number density on two dimensional melting may be interesting for future investigations.

For the experimental measurement of the kinetic temperature a velocity distribution function in two orthogonal directions has been calculated. For a better measurement of the distribution function, a video sequence of 100 frames has been chosen where the particle image velocimetry (PIV) analysis package, DAVIS 8 [28] is used to construct the velocity vector fields. Figure 9 shows the velocity distribution of our experimental data along the x- and y-directions for discharge parameters of $V_d = 310$ Volt and $P = 14$ Pa. The distribution function is found to reasonably well fit using a Maxwellian distribution (solid line) on the experimental data points in the figures. The kinetic dust temperature is calculated from the width of the measured distribution by using the formula $E = \frac{1}{2}m\langle v_{x,y}^2\rangle = \frac{1}{2}k_B T_{x,y}$. Figure 10 shows the measured kinetic temperature of the dust particles with background neutral pressure. It can be seen from the figure that at the lower pressure the temperature is higher. It is interesting to note that our measured temperature is twice the order of magnitude less than the previously reported temperature during the melting transition in rf plasma. A rapid fall in the temperature is observed with increasing pressure and above 13 Pa it decays slowly and then saturates at ~0.035 eV which is close to the room temperature. The decrease in the dust kinetic temperature at increasing pressure can be attributed to the collisional cooling of the dust particles by the increasing number of neutral particles.

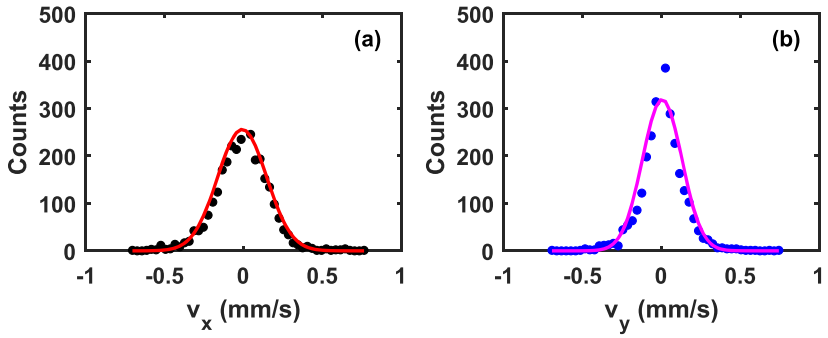

Figure 9. A typical distribution of velocities is depicted for (a) the x component, (b) the y component. The points depict the distribution of measured velocities, while the solid curve represents the fit of the Maxwellian velocity distribution.

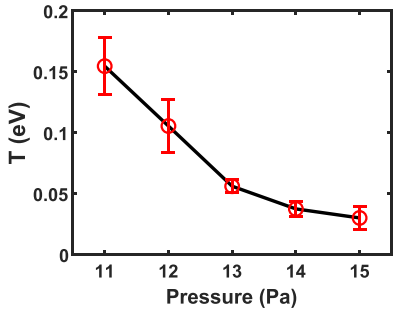

Figure 10. A plot of the kinetic temperature of the dust cloud as a function of the neutral gas pressure.

The experimental measurements that have been presented in this paper show strong evidence of a melting transition in a dc glow discharge dusty plasma. Here, we discuss some possible mechanisms that could be responsible for the heating of the dust particles. The most important experimental parameter in this study is the lowering of the neutral pressure and we consider how this could impact the properties of the dust particles. For example, work by Vaulina *et al* [29] predicts the dust charge fluctuation can play a role in increasing the dust kinetic temperature. The dust charge fluctuation is dependent on two parameters; particle charge and their mass. In order to estimate the dust charge, we have followed the procedure outlined in the paper by Khrapak *et al* [30] that estimates the charge based on its dependence on the ratio of the charge density of the particles to that of the ions, defined as Havnes parameter [31]

$$P = \frac{aT_e}{e^2}\frac{n_p}{n_0} \cong 695aT_e\frac{n_p}{n_0}, \tag{2}$$

where a is the particle radius (in μm), T_e is the electron temperature (in eV) and n_p and n_0 is the particle and plasma densities, respectively. When $P > 1$, the charge and floating potential are significantly diminished, while for $P \ll 1$ the charge and floating potentials approach the values for an isolated particle [4, 29]. Knowing the information of P, one can estimate the dimensionless charge ($z = e^2 Z_d / 4\pi\epsilon_0 a k_B T_e$) [30] and hence the corresponding charge residing on the particle, Q. For our range of pressure 15–11 Pascal and the corresponding measured parameters $T_e = (2.8–4.3)$ eV, $n_0 = (1.5–0.8) \times 10^{15}$ m^{-3}, $n_p = (2.45–1.35) \times 10^{10}$ m^{-3} [24], the dimensionless charge is estimated as $z \sim 2.25$ and the value of charge varies from 1833–2984 elementary charges. Therefore, this estimate suggests an increase of the particle charge, and subsequently the charge fluctuation, with decreasing neutral pressure—which could contribute to the heating of the dust particles [32, 33]. In addition to the charge fluctuation, the streaming ions also play a very important role in heating up the particles due to static and strong ion current in the dc glow discharge plasma. Ion streaming will increase with decreasing neutral pressure. Earlier modelling studies by Joyce *et al* [34] have shown that ion-dust streaming instabilities are an important mechanism that can lead to the heating of dust particles. However, the asymmetry of the electrodes and the presence of confining strips has helped in reducing the heating effects associated with ion streaming. It is noted that in the recent work by Hari *et al* [23], a detailed analysis of the experimental geometry of the DPEx device was performed to study the role of the asymmetric electrode configuration and the confinement strips on the stability of a plasma crystal. This work, in combination with the results presented in that paper, indicate that the experimental geometry plays a critical role in establishing a careful balance between

the ion streaming and the other forces on the dust particles that lead to a narrow region in parameter space where the plasma crystal can be formed in the DC glow discharge configuration. From the work presented here, it is clear that the small changes in those experimental parameters—through a combination of streaming and charge fluctuation effects—can lead to melting. Therefore, future studies should focus on carefully characterizing the ion dynamics in this experiment.

4. Conclusion

In conclusion, we present an experimental investigation on the melting transition of dust crystal in DC glow discharge plasma. An asymmetrical electrode configuration along with the confining strips facilitates the formation of a hexagonal crystalline structure at a pressure of 15 Pascal and a transition from solid state to a fluid state is observed at reducing gas pressure. The melting transition of the crystal is demonstrated by investigating the global and local structural properties of the dust cloud as a function of neutral pressure. The pair correlation shows a long—range order in the particle arrangement above 13 Pascal whereas ordering is reduced at lower pressure. The local variation in the structural dynamics of the particle cloud is examined by calculating the local bond order parameter Ψ_6 and defect fraction. The average bond order parameter is found to be maximum at 15 Pascal, $\Psi_6 = 0.87$ whereas it decreases to 0.4 at a pressure of 11 Pascal. The kinetic temperature is estimated from the velocity distribution of the particle. The measured kinetic dust temperature is found to be close to room temperature at higher pressure whereas it increases to 0.15 eV at lower pressure. We understand that the combined effect of charge fluctuation and ion streaming yield an increased dust temperature which induced melting of the crystalline structure at lower pressure. Our findings could be useful for exploring other innovative modifications in various DC glow discharge devices to make them suitable for the study of dusty plasma crystals and related phenomena.

Acknowledgments

Authors acknowledge the Institute for plasma research for providing the infrastructure. S. Jaiswal is thankful to Dr S. K. Mishra for valuable discussions and S. K. Pandey and R. Mukherjee for technical help. Additional funding support was provided by the NSF EPSCoR program (OIA-1655280).

ORCID iDs

S Jaiswal https://orcid.org/0000-0002-8447-2739

References

[1] Goertz C K 1989 *Rev. Geophys.* **27** 271
[2] Nakamura Y, Yokota T and Shukla P K (ed) 2000 *Frontiers in Dusty Plasmas* (Amsterdam: Elsevier Science)
[3] Selwyn G S, Singh J and Bennett R S 1989 *J. Vac Sci. Technol.* A **7** 2758
[4] Melzer A and Goree J 2008 Fundamentals of complex plasmas *Low Temperature Plasmas: Fundamentals, Technologies and Techniques* 2nd edn., ed R Hippler *et al* (Wiley-VCH Verlag GmbH) ch 6 pp 129–173
[5] Morfill G E and Ivlev A V 2009 *Rev. Mod. Phys.* **81** 1353
[6] Ikezi H 1986 *Phys. Fluids* **29** 1764
[7] Chu J H and Lin I 1994 *Phys. Rev. Lett.* **72** 4009
[8] Thomas H, Morfill G E, Demmel V, Goree J, Feuerbacher B and Möhlmann D 1994 *Phys. Rev. Lett.* **73** 652
[9] Melzer A, Homann A and Piel A 1996 *Phys. Rev.* E **53** 2757–66
[10] Schweigert I V, Schweigert V A, Melzer A and Piel A 2000 *Phys. Rev* E **62** 1238
[11] Schweigert V A, Schweigert I V, Melzer A, Homann A and Piel A 1998 *Phys. Rev. Lett.* **80** 5345
[12] Naumkin V N, Lipaev A M, Molotkov V I, Zhukhovitskii D I, Usachev A D and Thomas H M 2018 *Journal of Physics: Conf. Series* **946** 012144
[13] Knapek C A, Samsonov D, Zhdanov S, Konopka U and Morfill G E 2007 *Phys. Rev. Lett.* **98** 015004
[14] Couëdel L, Nosenko V, Ivlev A V, Zhdanov S K, Thomas H M and Morfill G E 2010 *Phys. Rev. Lett.* **104** 195001
[15] Meyer J K, Laut I, Zhdanov S K, Nosenko V and Thomas H M 2017 *Phys. Rev. Lett.* **119** 255001
[16] Jaiswal S, Hall T, LeBlanc S, Mukherjee R and Thomas E 2017 *Phys. Plasmas* **24** 113703
[17] Nunomura S, Samsonov D, Zhdanov S and Morfill G 2005 *Phys. Rev. Lett.* **95** 025003
[18] Fortov V E, Vaulina O S, Petrov O F, Vasiliev M N, Gavrikov A V, Shakova I A, Vorona N A, Khrustalyov Y V, Manohin A A and Chernyshev A V 2007 *Phys. Rev.* E **75** 026403
[19] Fortov V E, Nefedov A P, Torchinsky V M, Molotkov V I, Petrov O F, Samarian A A, Lipaev A M and Khrapak A G 1997 *Phys. Lett.* A **229** 317–22
[20] Maiorov S A, Ramazanov T S, Dzhumagulova K N, Jumabekov A N and Dosbolayev M K 2008 *Phys. Plasmas* **15** 093701
[21] Mitic S, Klumov B A, Konopka U, Thoma M H and Morfill G E 2008 *Phys. Rev. Lett.* **101** 125002
[22] Jaiswal S 2016 Nonlinear excitations in flowing complex plasmas *PhD Thesis* Homi Bhabha National Institute pp 64–6
[23] Hariprasad M G, Bandyopadhyay P, Arora G and Sen A 2018 *Phys. Plasmas* **25** 123704

[24] Jaiswal S, Bandyopadhyay P and Sen A 2015 *Rev. Sci. Instruments* **86** 113503
[25] Knapek C A, Ivlev A V, Klumov B A, Morfill G E and Samsonov D 2007 *Phys. Rev. Lett.* **98** 015001
[26] Knapek C 2000 Phase transitions in two-dimensional complex plasmas *PhD Thesis* Fakultät für Physik der Ludwig-Maximilians-Universität München ch 4 and 7
[27] Couëdel L, Nosenko V, Rubin-Zuzic M, Zhdanov S, Elskens Y, Hall T and Ivlev A V 2018 *Phys. Rev.* E **97** 043206
[28] DaVis (Data Visualization) Software, Version 8.0, LaVision GmbH. Göttingen, Germany 2013.
[29] Vaulina O S, Khrapak S A, Nefedov A P and Petrov O F 1999 *Phys. Rev.* E **60** 5959–64
[30] Khrapak S A, Thomas H M and Morfill G E 2010 *EPL* **91** 25001
[31] Havnes O, Aanesen T K and Melandsø F 1990 *J. Geophys. Res.* **95** 6581
[32] de Angelis U, Ivlev A V, Tsytovich V N and Morfill G E 2005 *Phys. Plasmas* **12** 052301
[33] de Angelis U 2006 *Phys. Plasmas* **13** 012514
[34] Joyce G, Lampe M and Ganguli G 2002 *Phys. Rev. Lett.* **88** 095006